

Theoretical study of the charge transport through C₆₀-based single-molecule junctions

S. Bilan,¹ L. A. Zotti,¹ F. Pauly,^{2,3} and J. C. Cuevas¹

¹*Departamento de Física Teórica de la Materia Condensada,
Universidad Autónoma de Madrid, E-28049 Madrid, Spain*

²*Institut für Theoretische Festkörperphysik and DFG Center for Functional Nanostructures,
Karlsruhe Institute of Technology, D-76131 Karlsruhe, Germany*

³*Molecular Foundry, Lawrence Berkeley National Laboratory, Berkeley, California 94720, USA*

(Dated: February 26, 2013)

We present a theoretical study of the conductance and thermopower of single-molecule junctions based on C₆₀ and C₆₀-terminated molecules. We first analyze the transport properties of gold-C₆₀-gold junctions and show that these junctions can be highly conductive (with conductances above $0.1G_0$, where $G_0 = 2e^2/h$ is the quantum of conductance). Moreover, we find that the thermopower in these junctions is negative due to the fact that the lowest unoccupied molecular orbital (LUMO) dominates the charge transport, and its magnitude can reach several tens of $\mu\text{V/K}$, depending on the contact geometry. On the other hand, we study the suitability of C₆₀ as an anchoring group in single-molecule junctions. For this purpose, we analyze the transport through several dumbbell derivatives using C₆₀ as anchors, and we compare the results with those obtained with thiol and amine groups. Our results show that the conductance of C₆₀-terminated molecules is rather sensitive to the binding geometry. Moreover, the conductance of the molecules is typically reduced by the presence of the C₆₀ anchors, which in turn makes the junctions more sensitive to the functionalization of the molecular core with appropriate side groups.

PACS numbers: 73.63.Rt, 73.61.Wp, 73.40.Jn, 85.65.+h

I. INTRODUCTION

The fullerene C₆₀ is attracting a lot of attention in the field of molecular electronics.¹ One reason is that the delocalization of the frontier orbitals of C₆₀ suggests that this molecule can be a good candidate to build highly conductive single-molecule junctions, a goal that remains elusive and that it has only been achieved with short molecules.^{2–6} On the other hand, it has been recently suggested that C₆₀ used as an anchoring group to bind molecules to the electrodes can improve the reproducibility of the conductance measurements in single-molecule junctions,⁷ which is a crucial issue in molecular electronics. The goal of this work is to further analyze these two different questions from a theoretical point of view.

The first experiment on individual C₆₀ molecules was reported by Joachim *et al.*⁸ Here, a scanning tunneling microscope (STM), with a tip made of tungsten, was used at room temperature to study the conductance of a C₆₀ molecule on an Au(110) surface. It was shown that in the contact regime this heterojunction has a conductance of $2.35 \times 10^{-4}G_0$, which is clearly lower than in the case of metallic atomic-size contacts. Since then, different groups have investigated experimentally the transport properties of C₆₀ molecular junctions, mainly with gold electrodes, and they have reported very different results. Thus for instance, Park *et al.*⁹ performed measurements in Au-C₆₀-Au junctions using the electromigration technique and depositing the C₆₀ molecules from a liquid solution. In this case, the conductance at low bias was found to be largely suppressed and the current-voltage characteristics were dominated by the Coulomb blockade phenomenon. A related experiment, but this time with a microfabricated break junction, showed a much higher

low-bias conductance (of the order of $0.1G_0$), which was attributed to the appearance of Kondo physics.¹⁰ A more systematic study of the low-bias conductance was carried out by Böhler *et al.*¹¹ In this case, the authors conducted low-temperature (10 K) break junction experiments in which the molecules were evaporated *in situ*. From the analysis of a conductance histogram, it was concluded that Au-C₆₀-Au junctions exhibit a preferred conductance value close $0.1G_0$. On the contrary, recent STM break junction experiments at room temperature have shown a very large spread of conductances with a certain preference for values around $5 \times 10^{-4}G_0$.¹²

The main evidence that C₆₀ junctions can have a rather high conductance has been provided by a series of controlled STM experiments with other electrode materials (different from gold) performed by Berndt and coworkers and which have been nicely backed up theoretically.^{13–16} Thus for instance, Néel *et al.*¹³ reported a controlled STM study in ultrahigh vacuum (UHV) in which C₆₀ molecules deposited onto copper surfaces exhibited conductance values of the order of $0.25G_0$ in the contact regime. It is also worth mentioning that Kiguchi¹⁷ reported break junction experiments at room temperature in UHV conditions in which a single C₆₀ molecule between Pt electrodes was shown to exhibit a conductance as high as $0.7G_0$.

Although the electronic and transport properties of C₆₀ metal-molecule-metal junctions have been addressed theoretically by numerous groups,^{13–16,18–23} studies of transport in C₆₀ junctions with gold electrodes, the most commonly used metal in molecular electronics, are surprisingly rather scarce.^{24,25} Moreover, those references explore only ideal contact geometries which may have little to do with those realized in the experiments. For

this reason, we present here an *ab initio* study of the charge transport in Au-C₆₀-Au junctions paying special attention to the role of the contact geometry. Our analysis, based on the combination of density function theory (DFT) and nonequilibrium Green's function techniques, shows that conductances above $0.1G_0$ are possible in realistic contact geometries. Moreover, motivated by very recent experiments,¹² we have investigated the thermopower of these junctions and found that this quantity is negative, as reported in Ref. 12, which is simply due to the fact that the low-bias transport is dominated by the C₆₀ LUMO. Furthermore, we have found that the thermopower varies significantly with the contact geometry, and its magnitude can reach several tens of $\mu\text{V/K}$, which is higher than in previously investigated molecules.^{26,27}

The second topic that we want to address in this work is the role of C₆₀ as an anchoring group. Some of the main challenges in the field of molecular electronics are related to the fabrication of single-molecule junctions with very well-defined transport properties and the ability to tune those properties at will. A strategy that is being pursued to achieve these goals is the use of suitable anchoring groups to bind the molecules to the metallic electrodes. The thiol (–SH) group is the most commonly used anchoring group, specially when the electrodes are made of gold, because of their high covalent bond strength.²⁸ However, the thiol group has been shown to lead to a large variety of binding geometries,^{29–31} which implies a large spread in the observed conductance values. Many different alternatives to the thiol group have been explored in recent years. For instance, Venkataraman and coworkers³² introduced the amine group (–NH₂) as an interesting possibility to obtain better defined values in the conductance histograms, which was attributed to a higher selectivity of amine-gold binding. Similar conclusions have been drawn in a recent analysis of nitrile-terminated (–C≡N) biphenyls.³³ The list of anchoring groups explored in molecular junctions increases steadily and the search for the “most” convenient group, leading to highly reproducible transport properties, has become one of the central issues in molecular electronics.^{3,34,35}

In this context, Martin *et al.*⁷ put forward the interesting idea of using C₆₀ as a new anchoring group. The idea is that C₆₀ offers a large contact area which, together with the high molecular symmetry, may reduce the spread of the conductance values. Moreover, this fullerene is known to strongly hybridize with metallic surfaces,³⁶ and, as explained above, it has been shown in different STM and break junction experiments that it can sustain a rather high conductance. Indeed, in Ref. 7 the electrical characteristics of 1,4-bis(fullero[c]pyrrolidin-1-yl)benzene (BDC60) (with C₆₀ anchor groups) were studied using gold microfabricated break junctions, and it was found that the conductance histograms exhibited more pronounced peaks than those obtained with 1,4-benzenediamine and 1,4-benzenedithiol. More recently, Leary *et al.*³⁷ have shown that the use of C₆₀ as anchoring group facilitates enormously the characterization of

single-molecule junctions in STM experiments under ambient conditions and it allows to establish unambiguously the conductance of the molecule under study.

These experimental results are promising, but it remains to be explored whether the use of C₆₀ as a terminal group still allows, for instance, for the possibility to chemically tune the conductance by an appropriate functionalization of the molecular core, as it has been demonstrated with other anchoring groups.^{33,38–41} In other words, the main role of an anchoring group must be to provide the chemical link to the electrodes without modifying the essential properties of the molecular backbone. In this sense, it remains to be shown whether or not C₆₀ is too invasive to be used as an anchoring group.

Besides the results for the pure C₆₀, we also present a study of the transport properties of molecular junctions based on C₆₀-terminated molecules: BDC60 and several derivatives. Our DFT-based analysis aims at addressing two main questions: (i) Does C₆₀ reduce the spread in conductance values found with other anchoring groups? and (ii) Is C₆₀ too invasive to be used as a suitable anchoring group? Our results suggest that the conductance and thermopower of C₆₀-terminated molecules are still quite sensitive to the binding geometry and we expect a large spread of values in typical STM and break junction experiments. On the other hand, our results indicate that C₆₀ may reduce the electron communication between the molecular core and the metallic electrodes, leading to a reduction of the conductance. However, this reduction of the effective metal-molecule coupling and the fact that the frontier orbitals lie relatively close to the Fermi energy lead to a notable increase in the sensitivity of the junctions to the functionalization of the molecular backbone, as compared with thiol or amine groups.

The rest of the paper is organized as follows. In the next section we briefly describe the methodology employed to compute the transport properties of single-molecule junctions. Then, in Sec. III we present a detailed analysis of the conductance and thermopower of Au-C₆₀-Au junctions. Sec. IV is devoted to the analysis of junctions with BDC60 molecules modified by the inclusion of several side groups. The results for the conductance and thermopower of these junctions are compared with those obtained using thiol and amine as anchoring groups. Finally, we summarize the main conclusions of this work in Sec. V.

II. METHODOLOGY

Our main goal is to describe the transport properties of single-molecule junctions based on C₆₀ molecules and C₆₀-terminated compounds. For this purpose, we employed the DFT-based transport method described in detail in Ref. 42, which is built upon the quantum-chemistry code TURBOMOLE 6.1.⁴³ In this method, the first step is the description of the electronic structure of the molecular junctions within DFT. In all our calcu-

lations we used the BP86 functional⁴⁴ and the def-SVP basis set.⁴⁵ In order to construct the junction geometries, we first relaxed the molecules in the gas phase. Then, the molecular junctions were constructed by placing the relaxed molecules between two finite clusters of 20 (or 19) gold atoms and performing a new geometry optimization. In this optimization, the molecule and the 4 (or 3) outermost gold atoms on each side were relaxed, while the other gold atoms were kept frozen. Subsequently, the size of the gold clusters was extended to around 63 atoms on each side in order to describe the metal-molecule charge transfer and the energy level alignment correctly.

The final step in our method is to transform the information about the electronic structure of the junctions obtained within DFT into the different transport properties. This is done using nonequilibrium Green's function techniques, as described in detail in Ref. 42. In the coherent transport regime, and following the spirit of the Landauer approach, the low-temperature linear conductance is given by $G = G_0 \tau(E_F) = G_0 \sum_i \tau_i(E_F)$, where $G_0 = 2e^2/h$ is the quantum of conductance, $\tau(E_F)$ is the junction transmission at the Fermi energy, E_F , and $\{\tau_i(E)\}$ are the transmission coefficients, *i.e.*, the energy-dependent eigenvalues of the transmission matrix. The second transport property of interest in this work is the thermopower, which within the coherent transport regime is given by

$$S = -\frac{K_1(T)}{eTK_0(T)}, \quad (1)$$

with $K_n(T) = \int dE (E - \mu)^n \tau(E) [-\partial_E f(E, T)]$, where μ is the electrochemical potential and $f(E, T) = [1 + \exp[(E - \mu)/k_B T]]^{-1}$. We shall compute the thermopower at room temperature ($T = 300$ K), and in all the examples discussed here one can still use the low-temperature expansion of Eq. (1), which is given by

$$S = -\frac{\pi^2 k_B^2 T}{3e} \frac{\tau'(E_F)}{\tau(E_F)}. \quad (2)$$

Here, the prime denotes a derivative with respect to energy. Thus, the thermopower measures the logarithmic first derivative of the transmission function at $E = E_F$. The sign of this quantity carries information about the location of the Fermi energy within the gap of a molecular junction.^{46,47}

III. CONDUCTANCE AND THERMOPOWER OF GOLD-C₆₀-GOLD JUNCTIONS

This section is devoted to the analysis of the transport properties of Au-C₆₀-Au junctions, which will also serve us as a reference for the study of the C₆₀-terminated molecules. Let us start our analysis by recalling the electronic structure of C₆₀ in the gas phase. Within our DFT approach, and in agreement with Ref. 24, we find that the highest occupied molecular orbital (HOMO) is

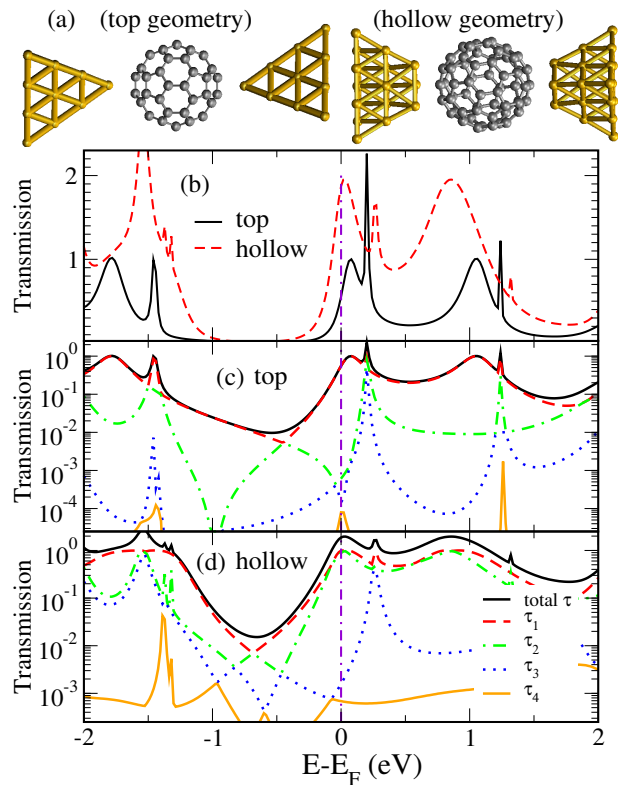


FIG. 1. (Color online) (a) Two ideal Au-C₆₀-Au junctions with top (left) and hollow (right) binding geometries. (b) The transmission as a function of energy for the two geometries in (a). (c-d) In these two panels the solid line corresponds to the total transmission, while the others correspond to the contribution of the individual transmission coefficients as a function of energy.

five-fold degenerate, while the LUMO is three-fold degenerate (at -5.90 and -4.26 eV, respectively). These energies have to be compared with the Fermi energy of gold, which in our calculations is -5.0 eV. In order to elucidate how the electronic transport takes place through a C₆₀ molecule coupled to gold electrodes, we first consider two ideal geometries in which the molecule is bound to the electrodes in a top and in a hollow position, see Fig. 1(a). These geometries have been constructed as follows. We first relaxed the molecule on top of a single cluster, then we added a second cluster symmetrically at the other end, and finally we relaxed again the whole junction, as described in the previous section. In the top position, we find that the apex gold atom binds to two carbon atoms of a 6:6 bond, each C-Au distance being around 2.45 Å. This geometry is consistent with that reported in Ref. 21 for various C₆₀-gold nanocontacts. In the hollow position, similar to that explored in Ref. 23, the three-Au-atom terrace is facing one carbon atom and C-Au distances are in the range 2.3 - 2.4 Å.

In Fig. 1(b-d) we show both the total transmission and its channel decomposition as a function of energy

for these two ideal contact geometries. The first thing to notice is that the conductance, determined by the transmission at the Fermi energy, is very high as compared with other organic molecules of similar length, $0.55G_0$ and $1.85G_0$ for the top and hollow position, respectively. In both cases the low-bias conductance is dominated by the LUMO of the molecule, as it has been found in STM experiments of C_{60} on Au surfaces (see e.g. Ref. 48). For the top position, we find that the transmission at the Fermi energy is largely dominated by a single channel which originates from one of the LUMOs of the molecule, which is split from the other two and is shifted to lower energies due to its better coupling to the electrodes. For the hollow-type geometry, we find that two conduction channels give a significant contribution to the low-bias conductance. These channels originate from two of the LUMOs, which in this case are more strongly coupled to the electrodes than in the top geometry due to the higher number of C atoms in direct contact with the electrode atoms. This is simply the reason for the higher conductance of this geometry, which agrees with the findings of Ref. 15, where it was shown (both experimentally and theoretically) that the conductance of a C_{60} junction increases with the number of atoms in contact with the molecule. Let us also mention that conductances above $1G_0$ have also been reported in theoretical studies of C_{60} -junctions with Al,^{18,19} Au,²⁴ and Cu¹⁴ electrodes when the leads are similar to ideal surfaces, *i.e.*, with a high Au- C_{60} coordination.

The calculations discussed above suggest that Au- C_{60} -Au junctions can have a conductance comparable to metallic atomic-size contacts. However, the ideal geometries considered so far should provide a rough estimate for the expected conductance values since it is unlikely to realize experimentally contacts with such a high degree of symmetry. Thus, a more direct comparison with the experiments requires a detailed analysis of the junction formation and of the evolution of the conductance during the stretching of the contacts. This is precisely what we have done, as we now proceed to explain. In order to simulate the junction formation, we started with a geometry in which the molecule is positioned laterally with respect to the gold-gold axis and we used gold clusters terminated with a single Au atom, Fig. 2(a). Then, the gold electrodes were separated step-wise (in steps of ~ 1 Å) and the junction geometry was relaxed in every step. This protocol was repeated until the junction was broken and the molecule lost contact with the electrodes. To characterize the junction during the stretching process, we computed different quantities such as the binding energy of the junction, the Mulliken charges in the C_{60} molecule, the linear conductance, and the thermopower at room temperature. The results are shown in panels (b) to (e) of Fig. 2. Notice that in panel (d) we have also included the conductance of a Au-Au junction with the same distance separation to estimate how much current is flowing directly from gold to gold (bypassing the molecule) in the different stages of the elongation

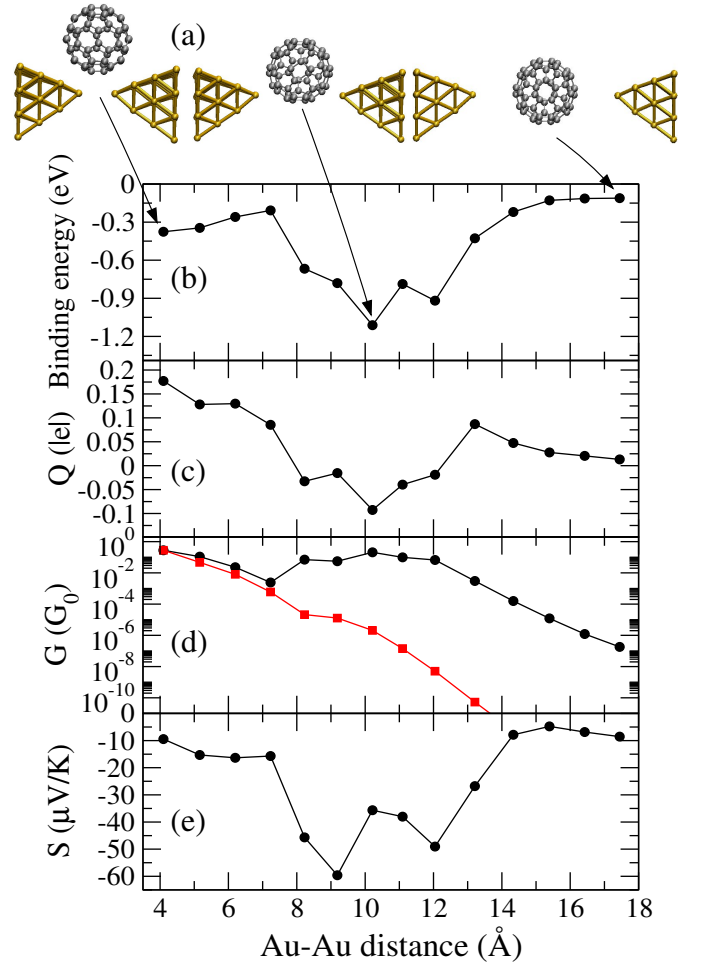


FIG. 2. (Color online) (a) Some representative geometries of the stretching simulation of a Au- C_{60} -Au junction. They correspond to Au-Au distances (distance between the Au tips) of 4.2 Å, 10.2 Å, and 17.5 Å. The other panels show the following quantities during the stretching process: (b) binding energy of the junction, (c) charge on the C_{60} molecule, (d) conductance of the Au- C_{60} -Au junction (circles) and, for comparison, conductance of a Au-Au junction with the same distance separation (squares), and (e) thermopower at room temperature.

process.

In our simulation, after the first steps, the molecule rotates and then it places itself in the middle of the junction adopting a geometry in which the top gold atom is bound to a single C atom, see central geometry of Fig. 2(a). This structure, which is the most stable one with a binding energy close to 1 eV, differs from the very symmetric top geometry in Fig. 1(a). In this geometry the Au- C_{60} interaction is maximized by the proximity of the side surface of the Au cluster. This is consistent with a related analysis reported in Ref. 20. Then, after further stretching, the center of the molecule is aligned with the junction axis and the molecule remains there until the rupture of the contact. In the Au-Au distance range 8-12 Å,

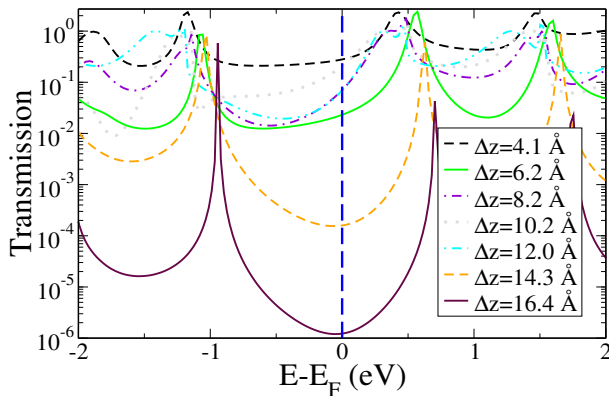


FIG. 3. (Color online) Transmission as a function of energy for the Au-C₆₀-Au junctions shown in Fig. 3(a). The different curves correspond to different elongation stages, as indicated in the legend (Δz refers to the Au-Au distance).

where the binding energy is maximum in magnitude, the molecule is negatively charged and the conductance exhibits a “plateau” with values between 0.07 and $0.2G_0$, which is consistent with the experiments of Ref. 11. At an Au-Au distance of ~ 12 Å, the contact breaks, as suggested by the evolution of the binding energy, and the conductance starts to decrease exponentially, while there is a tiny positive charge in the molecule.

The thermopower results shown in Fig. 2(e) deserve special attention in view of the recent experimental results reported in Ref. 12. In that work, thermopower measurements of fullerene-metal junctions were performed at room temperature with a STM break junction technique. In particular, for Au-C₆₀-Au junctions a preferred value of -14.5 ± 1.2 $\mu\text{V/K}$ was found, the minus sign suggesting that the LUMO dominates the conduction. As we show in Fig. 3, where we display the transmission curves of Au-C₆₀-Au junctions at different elongation stages in the simulation, the low-bias transport is dominated by the LUMO of the molecule at any distance. As a consequence, the thermopower is negative at any stage of the elongation process, see Fig. 2(e), and in particular, its value for the most stable geometry is approximately -35 $\mu\text{V/K}$, which is a factor two larger than in the experiment. Let us also mention that for the ideal junctions of Fig. 1(a) we obtain a thermopower of -19.37 $\mu\text{V/K}$ for the hollow geometry and a value of -91.62 $\mu\text{V/K}$ for the top one. This big difference between these two geometries is due to the fact that the transport takes place in an almost on-resonant situation.

To conclude this section, it is worth commenting that in our simulations we have not taken into account the van der Waals interactions. In this sense, the binding distances might not be exact. Dispersion forces play a role in the interaction between C₆₀ and gold.⁴⁹ However, the Au-C₆₀ binding is known to be mainly covalent with some ionic character.^{49,50,52} This is corroborated by the fact that, during our simulated elongation, the molecule

is pulled in between the electrodes, due to the chemical interaction.

IV. C₆₀ AS AN ANCHORING GROUP

We now analyze the role of C₆₀ as an anchoring group in molecular junctions. We have seen in the previous section that this molecule can sustain a rather high conductance, which suggests that C₆₀ can, in principle, provide a very efficient electronic communication, when used as an anchoring group. To explore this idea, let us first study the transport through a 1,4-bis(fullero[c]pyrrolidinyl)benzene (BDC60) molecule, see Fig. 4, in which a phenyl ring is connected to two fullerenes on two opposite sides via a pyrrolidine group (in a so-called “dumbbell” fashion). We have chosen this molecule for several reasons. First, it has been investigated both experimentally⁷ and theoretically,^{51,52} which allows us to establish a comparison with our results. Second, the transport through the central moiety (a phenyl ring) can be analyzed with other anchoring groups, which is necessary to determine the quality of C₆₀ as a terminal group.

Our DFT calculations of the electronic structure of the isolated BDC60 molecule show that its HOMO appears at -4.7 eV and that it is localized on the central part of the molecule, while the two-fold degenerate LUMO is localized on the C₆₀’s, as displayed in Fig. 4. These two LUMOs are the lowest in energy of a series of six levels (ranging from -4.18 to -3.87 eV) which originate from the interaction between the three LUMO orbitals of each C₆₀, as explained in detail in Ref. 52. In agreement with this reference, we find that the nitrogen atoms are displaced

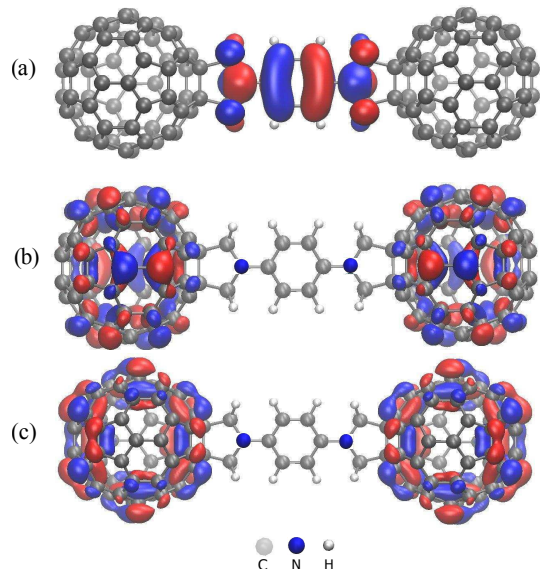


FIG. 4. (Color online) (a) HOMO and (b-c) two-fold degenerate LUMO of the BDC60 in the gas phase.

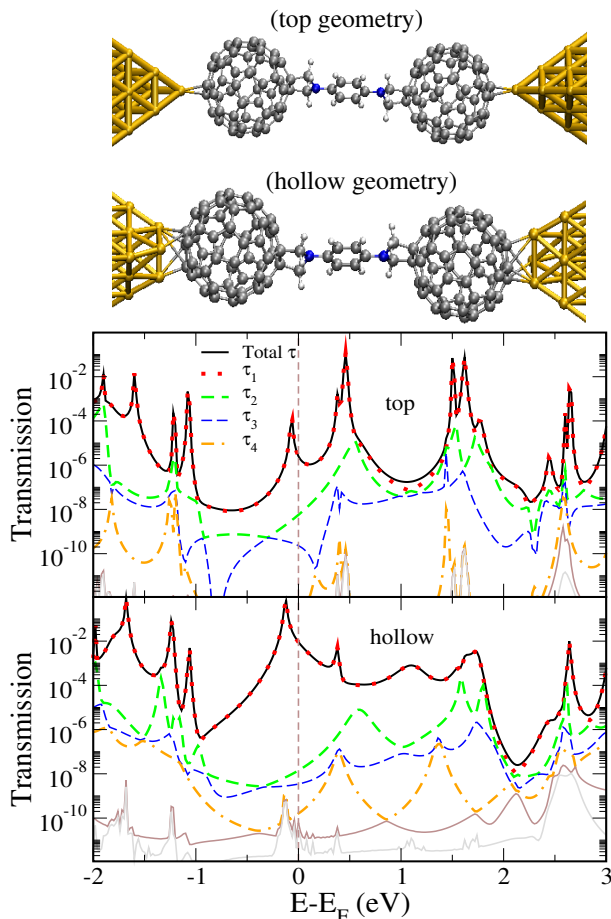


FIG. 5. (Color online) Total transmission and individual transmission coefficients as a function of energy for the two Au-BDC60-Au junction geometries shown in the upper part (top and hollow positions).

from the phenyl ring plane.

Turning now to the analysis of the Au-BDC60-Au junctions, we have again studied the conductance of two different types of geometries, a hollow and a top binding geometry, see the upper part of Fig. 5. In the hollow position, the three top Au atoms are bound to four C atoms, while in the top position, the apex gold atom is bound to two C atoms of a 6:6 bond. In Fig. 5 we show the results for the total transmission and the channel decomposition as a function of energy for both geometries. In both cases, the transmission close to the Fermi energy is dominated by a single channel and the resonance just below E_F originates from the HOMO of the molecule. In spite of the fact that the HOMO is pinned very close to the Fermi energy in both cases, the conductance is equal to $9.0 \times 10^{-3} G_0$ for the hollow position, while it is $2.5 \times 10^{-6} G_0$ for the top geometry. These values should be compared with the preferential value of $3 \times 10^{-4} G_0$ reported in the experiments of Ref. 7, although a large spread of conductance values was also found there. We attribute the low values of the conductance (as compared

	HOMO (eV)				LUMO (eV)			
	CH ₃	H	F	Cl	CH ₃	H	F	Cl
S	-4.82	-4.96	-5.47	-5.46	-1.23	-1.42	-1.75	-2.13
NH ₂	-3.88	-5.48	-5.92	-5.93	-0.52	-1.16	-1.67	-1.97
C ₆₀	-5.04	-4.70	-5.24	-5.56	-4.16	-4.18	-4.19	-4.18

TABLE I. HOMO and LUMO energies of the molecules (in gas phase) based on the phenyl unit and different anchoring and side groups.

to the C₆₀ junctions) and the difference between the two geometries to the weak effective coupling of the phenyl ring to the C₆₀ molecules, which is quite apparent in the small width of the transmission resonances. In other words, the phenyl-C₆₀ effective coupling is the actual bottleneck in these junctions and its weakness makes the conductance very sensitive to the exact level alignment and to the metal-molecule coupling.

Let us compare our results for the BDC60 molecule with other theoretical results published recently. First, we find that the current is mainly carried by the HOMO of the BDC60, while in Ref. 52 it was found that the transport is dominated by the LUMO. Let us stress that we have confirmed the level alignment described above by test calculations with even larger gold clusters (116 atoms). The discrepancy between these results may be due to differences in the electrodes' shape (in Ref. 52 the electrodes were modeled as ideal surfaces) and to the periodic boundary conditions applied in their model.⁵⁵ Second, in Ref. 52 it was claimed that the conductance of the Au-BDC60-Au junctions is not very sensitive to the binding geometry, while we find a large difference between the top and hollow geometries. We attribute this discrepancy to the fact that in that reference no binding with undercoordinated Au atoms was considered. On the other hand, in Ref. 51 it was stated that the weak coupling and the insufficient conjugation throughout the three parts of this molecule is detrimental for the electronic transmission. Although our results can not be directly compared with those of Ref. 51 (supporting LUMO transport), we agree in observing that the peaks corresponding to the frontier orbitals (HOMO and LUMO) appear narrower and lower than in the transmission curve of C₆₀.

After studying BDC60, we want to address the issue of whether or not the conductance of this dumb-bell molecule can be chemically tuned by functionalizing the phenyl unit, as it is known to be possible with other anchoring groups. To this aim, we have investigated three different substituents: CH₃, F, and Cl, and we shall compare the results with those obtained employing two other widely used anchoring groups, namely thiol (-SH) and amine (-NH₂). The CH₃ group is known to be electron-donating, while F and Cl are electron-withdrawing groups, and indeed for the molecules with thiol and amine anchoring groups the HOMO and LUMO are pushed upward in energy when the molecule is functionalized with CH₃, while they are pulled downward with F and Cl, see Table I. However, in the case of the

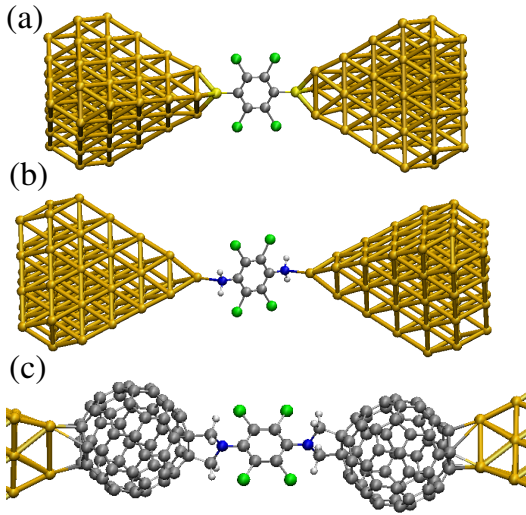


FIG. 6. (Color online) Geometries of the studied molecular junctions with a phenyl ring functionalized with chlorine and attached to the gold electrodes via (a) thiol, (b) amine, and (c) C_{60} groups.

dumbbell molecules this trend is not reproduced. The LUMO is not affected by the presence of the side groups, as expected since it resides in the C_{60} s, and the HOMO is shifted to lower energies also in the presence of the CH_3 group, see Table I. Moreover, in this case the functionalization causes a distortion of the central part, due to the interaction between the pyrrolydine and the substituents. This distortion, which does not occur in the case of SH and NH_2 because of their lower steric hindrance, is responsible for the unusual behavior of the CH_3 side group.

As an illustration, in Fig 6 we show the molecular junctions for the three different anchoring groups and with Cl functionalization. We choose a top binding geometry for NH_2 (let us remind that the amine group only binds to undercoordinated Au sites) and a hollow one for SH and C_{60} . In Fig 7 we show the transmission curves for all molecules with different anchoring groups, as well as a comparison of the conductance values in the lowest panel. The first thing to notice is that for all anchoring groups, the relative energy positions of the frontier orbitals upon side functionalization reproduce the trends observed in the gas phase. For thiol- and amine-terminated molecules the current flows through the HOMO, consistent with what was found for tolane molecules with the same anchoring groups.³⁴ Concerning the conductance values, the functionalization has no dramatic effect in the cases of the thiol and amine group, see lower panel of Fig 7. The shift in the position of the frontier orbitals is more apparent in the values of the thermopower, which are shown in Table II for all the molecules. In this table one can see the confirmation of the naive expectation that says that when the transport is dominated by the

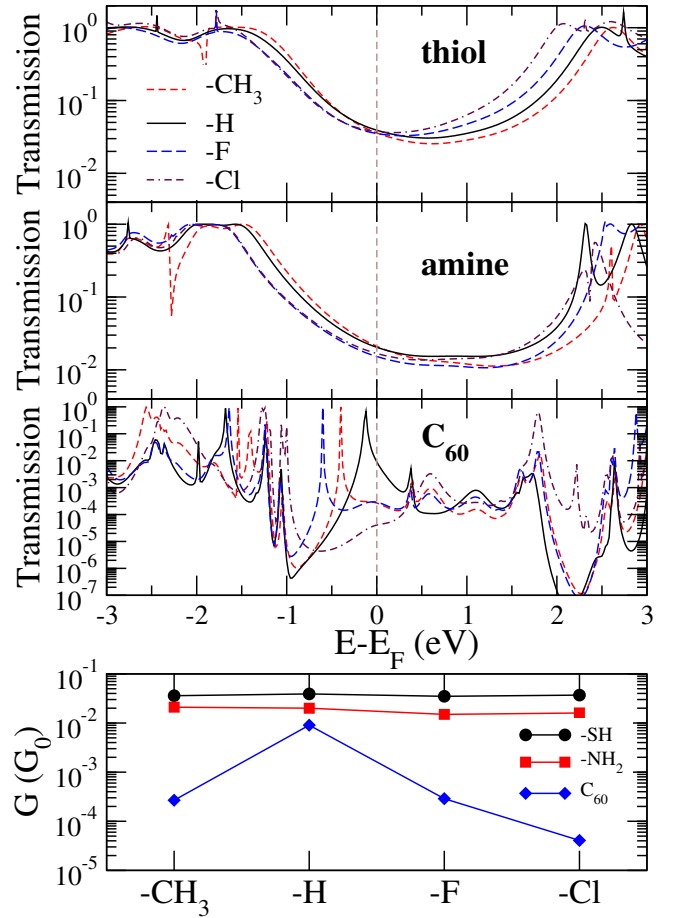


FIG. 7. (Color online) From top to bottom: Transmission curves for molecules anchored via thiol, amine, and C_{60} groups, and conductance values for all the junctions.

HOMO, the thermopower increases when the HOMO is shifted to higher energies, and it decreases when this orbital is pushed to lower energies. Moreover, it is worth stressing that the thermopower for the benzenedithiol molecules has been measured by Baheti *et al.*²⁷ and our results are in good quantitative agreement.

As one can see in Fig 7, the effect of the side groups is much more pronounced in the case of the C_{60} -terminated molecules. In particular, the functionalization in this case lowers considerably the conductance. The main reason for that is that the transmission resonance that

	Thermopower ($\mu V/K$)			
	CH_3	H	F	Cl
S	8.36	7.31	5.18	4.03
NH_2	8.96	6.98	6.29	5.64
C_{60}	18.90	96.74	13.0	-12.95

TABLE II. Thermopower of the different molecular junctions analyzed in Fig. 7 with different side groups and anchoring groups.

dominates the transport, and which is associated to the HOMO of the molecule, is much narrower for this anchoring group and therefore, it is much more sensitive to the shift induced by the side group. Notice also that in the case of the Cl group, the conductance is indeed dominated by the LUMO of the molecule due to the strong energy shift of the HOMO in this case. This fact is reflected in a change of sign in the thermopower (see Table II), which is something that does not occur for the other two anchoring groups.

V. CONCLUSIONS

In summary, we have presented a DFT-based analysis of the conductance and thermopower of individual C_{60} and C_{60} -terminated molecules with gold electrodes. We have shown, in agreement with several experiments, that Au- C_{60} -Au junctions can have a rather high conductance above $0.1G_0$ for realistic geometries. Moreover, we have found that the transport through C_{60} takes place through its LUMO, which leads to a negative thermopower in agreement with recent measurements. The fact that the LUMO lies relatively close to the Fermi energy, which means in practice that the energy derivative of the transmission at the Fermi energy is rather large, leads to a rather high thermopower in comparison with other organic molecules.

On the other hand, to investigate the use of C_{60} as an anchoring group, we have first studied the transport through Au-BDC60-Au junctions and found that the conductance is rather sensitive to the binding geometry. Furthermore, we have found that the conductance is decreased, as compared with the C_{60} junctions, due

to the poor electronic communication between the C_{60} 's and the molecular core (phenyl unit). Then, in order to study whether C_{60} as a terminal group is too invasive, we have analyzed several BDC60 derivatives which differ in the presence of a side group in the phenyl unit (Cl, F, and CH_3), and we have compared the results with those obtained using thiol and amine anchoring groups. Our results indicate that the BDC60-based junctions are much more sensitive to the functionalization, *i.e.* the changes in the conductance and in the thermopower induced by the side groups are much more significant in the case of the molecules with C_{60} as anchoring group.

So in short, our study supports the idea that C_{60} is a good conductor and it suggests that it can be used as a convenient anchoring group to study typical effects related to the chemical modification of the molecules: role of side groups, degree of conjugation, length dependence, etc. However, C_{60} does not seem to resolve the usual problem related to the spread of conductance values. Moreover, in dumbbell molecules like BDC60, beside the substituent-related shifting effect, also configurational changes due to steric repulsions can play an important role.

VI. ACKNOWLEDGMENTS

We thank T. Frederiksen, G. Foti, E. Leary, and E. Scheer for fruitful discussions. S.B, L.A.Z. and J.C.C. were funded by the EU through the network BI-MORE (MRTN-CT-2006-035859) and by the Comunidad de Madrid through the program NANOBIOIMAGNET S2009/MAT1726. F.P. acknowledges funding through a Young Investigator Group and the DFG Center for Functional Nanostructures (Project C3.6).

-
- ¹ J. C. Cuevas and E. Scheer, *Molecular Electronics: An Introduction to Theory and Experiment*, (World Scientific, Singapore, 2010).
 - ² R. H. M. Smit, Y. Noat, C. Untiedt, N. D. Lang, M. C. van Hemert, J. M. van Ruitenbeek, *Nature* **419**, 906 (2002).
 - ³ M. Kiguchi, O. Tal, S. Wohlthat, F. Pauly, M. Krieger, D. Djukic, J. C. Cuevas, J. M. van Ruitenbeek, *Phys. Rev. Lett.* **101**, 046801 (2008).
 - ⁴ Z.-L. Cheng, R. Skouta, H. Vázquez, J. R. Widawsky, S. Schneebeli, W. Chen, M. S. Hybertsen, R. Breslow, L. Venkataraman, *Nature Nanotech.* **6**, 353 (2011).
 - ⁵ W. Chen, J. R. Widawsky, H. Vázquez, S. T. Schneebeli, M. S. Hybertsen, R. Breslow, L. Venkataraman, *J. Am. Chem. Soc.* **133**, 17160 (2011).
 - ⁶ Y. Kim, T. Pietsch, A. Erbe, W. Belzig, and E. Scheer, *Nano Lett.* **11**, 3734 (2011).
 - ⁷ C. A. Martin, D. Ding, J. K. Sørensen, T. Bjørnholm, J. M. van Ruitenbeek, and H. S. J. van der Zant, *J. Am. Chem. Soc.* **130**, 13198 (2008).
 - ⁸ C. Joachim, J. K. Gimzewski, R. R. Schlittler, C. Chavy, *Phys. Rev. Lett.* **74**, 2102 (1995).
 - ⁹ H. Park, J. Park, A. K. L. Lim, E. H. Anderson, A. P. Alivisatos, and P. L. McEuen, *Nature (London)* **407**, 57 (2000).
 - ¹⁰ J. J. Parks, A. R. Champagne, G. R. Hutchison, S. Flores-Torres, H. D. Abruña, and D. C. Ralph, *Phys. Rev. Lett.* **99**, 026601 (2007).
 - ¹¹ T. Böhler, A. Edtbauer, and E. Scheer, *Phys. Rev. B* **76**, 125432 (2007).
 - ¹² S. K. Yee, J. A. Malen, A. Majumdar, R. A. Segalman, *Nano Lett.* **11**, 4089 (2011).
 - ¹³ N. Néel, J. Kröger, L. Limot, T. Frederiksen, M. Brandbyge, and R. Berndt, *Phys. Rev. Lett.* **98**, 065502 (2007).
 - ¹⁴ G. Schull, T. Frederiksen, M. Brandbyge, and R. Berndt, *Phys. Rev. Lett.* **103**, 206803 (2009).
 - ¹⁵ G. Schull, T. Frederiksen, A. Arnau, D. Sánchez-Portal, and R. Berndt, *Nat. Nanotech.* **6**, 23 (2011).
 - ¹⁶ G. Schull, Y. J. Dappe, C. González, H. Bulou, and R. Berndt, *Nano Lett.* **11**, 3142 (2011).
 - ¹⁷ M. Kiguchi, *Appl. Phys. Lett.* **95**, 073301 (2009).
 - ¹⁸ J. J. Palacios, A. J. Pérez-Jiménez, E. Louis, and J. A. Vergés, *Phys. Rev. B* **64**, 115411 (2001).

- ¹⁹ J. J. Palacios, A. J. Pérez-Jiménez, E. Louis, and J. A. Vergés, *Nanotech.* **12**, 160 (2001).
- ²⁰ R. Stadler, S. Kubatin, and T. Bjørnholm, *Nanotech.* **18**, 165501 (2007).
- ²¹ M. K. Shukla, M. Dubey, and J. Leszczynski, *ACS Nano* **2**, 227 (2008).
- ²² E. Abad, C. González, J. Ortega, and F. Flores, *Org. Electron.* **11**, 332 (2010).
- ²³ E. Abad, J. I. Martínez, J. Ortega, and F. Flores, *J. Phys.: Condens. Matter* **22**, 304007 (2010).
- ²⁴ T. Ono and K. Hirose, *Phys. Rev. Lett.* **98**, 026804 (2007).
- ²⁵ X. Zheng, Z. Dai, and Z. Zeng, *J. Phys.: Condens. Matter* **21**, 145502 (2009).
- ²⁶ P. Reddy, S.-Y. Jang, R. Segalman, A. Majumdar, *Science* **315**, 1568 (2007).
- ²⁷ K. Baheti, J. A. Malen P. Doak, P. Reddy, S.-Y. Jang, T. D. Tilley, A. Majumdar, R. A. Segalman, *Nano Lett.* **8**, 715 (2008).
- ²⁸ F. Chen, X. Li, J. Hihath, Z. Huang, N. J. Tao, *J. Am. Chem. Soc.* **128**, 15874 (2006).
- ²⁹ K. H. Müller, *Phys. Rev. B* **73**, 045403 (2006).
- ³⁰ C. Li, I. Pobelov, T. Wandlowski, A. Bagrets, A. Arnold, F. Evers, *J. Am. Chem. Soc.* **130**, 318 (2008).
- ³¹ M. Bürkle, J. K. Viljas, A. Mishchenko, D. Vonlanthen, G. Schön, M. Mayor, T. Wandlowski, and F. Pauly, *Phys. Rev. B* **85**, 075417 (2012).
- ³² M. S. Hybertsen, L. Venkataraman, J. E. Klare, A. C. Whalley, M. L. Steigerwald, C. J. Nuckolls, *J. Phys.: Condens. Matter* **20**, 374115 (2008).
- ³³ A. Mishchenko, L. A. Zotti, D. Vonlanthen, M. Bürkle, F. Pauly, J. C. Cuevas, M. Mayor, and T. Wandlowski, *J. Am. Chem. Soc.* **133**, 184 (2011).
- ³⁴ L. A. Zotti, T. Kirchner, J. C. Cuevas, F. Pauly, T. Huhn, E. Scheer, and A. Erbe, *Small* **6**, 1529 (2010).
- ³⁵ M. Dell'Angela, G. Kladnik, A. Cossaro, A. Verdini, M. Kamenetska, I. Tamblyn, S. Y. Quek, J. B. Neaton, D. Cvetko, A. Morgante, L. Venkataraman, *Nano Lett.* **10**, 2470 (2010).
- ³⁶ C. Rogero, J. I. Pascual, J. Gómez-Herrero, and A. M. Baró, *J. Chem. Phys.* **116**, 832 (2002).
- ³⁷ E. Leary, M. T. González, C. van der Pol, M. R. Bryce, S. Filippone, N. Martín, G. Rubio-Bollinger, and N. Agrait, *Nano Lett.* **11**, 2236 (2011).
- ³⁸ L. Venkataraman, J. E. Klare, C. Nuckolls, M. S. Hybertsen, M. L. Steigerwald, *Nature* **442**, 904 (2006).
- ³⁹ L. Venkataraman, Y. S. Park, A. C. Whalley, C. Nuckolls, M. S. Hybertsen, and M. L. Steigerwald, *Nano Lett.* **7**, 502 (2007).
- ⁴⁰ E. Leary, S. J. Higgins, H. van Zalinge, W. Haiss and R. J. Nichols, *Chem. Commun.*, 3939 (2007).
- ⁴¹ A. Mishchenko, D. Vonlanthen, V. Meded, M. Bürkle, C. Li, I. V. Pobelov, A. Bagrets, J. K. Viljas, F. Pauly, F. Evers, M. Mayor, T. Wandlowski, *Nano Lett.* **10**, 156 (2010).
- ⁴² F. Pauly, J. K. Viljas, U. Huniar, M. Häfner, S. Wohlthat, M. Bürkle, J. C. Cuevas, G. Schön, *New J. Phys.* **10**, 125019 (2008).
- ⁴³ R. Ahlrichs, M. Bär, M. Häser, H. Horn, and C. Kölmel, *Chem. Phys. Lett.* **162**, 165 (1989).
- ⁴⁴ J. P. Perdew, *Phys. Rev. B* **33**, 8822 (1986).
- ⁴⁵ A. Schäfer, H. Horn, and R. Ahlrichs, *J. Chem. Phys.* **97**, 2571 (1992).
- ⁴⁶ M. Paulsson and S. Datta, *Phys. Rev. B* **67**, 241403 (2003).
- ⁴⁷ F. Pauly, J. K. Viljas, J. C. Cuevas, *Phys. Rev. B* **78**, 035315 (2008).
- ⁴⁸ X. Lu, M. Grobis, K. H. Khoo, S. G. Louie, and M. F. Crommie, *Phys. Rev. B* **70**, 115418 (2004).
- ⁴⁹ I. Hamada and M. Tsukada, *Phys. Rev. B* **83**, 245437 (2011).
- ⁵⁰ L. Wang and H. Cheng, *Phys. Rev. B* **69**, 165417 (2004).
- ⁵¹ J. K. Sørensen, J. Fock, A. H. Pedersen, A. B. Petersen, K. Jennum, K. Bechgaard, K. Kilsa, V. Geskin, J. Cornil, T. Bjørnholm, and M. B. Nielsen, *J. Org. Chem.* **76**, 245 (2011).
- ⁵² T. Markussen, M. Settnes, and K. S. Thygesen, *J. Chem. Phys.* **135**, 144104 (2011).
- ⁵³ R. N. Wang, X. H. Zheng, L. L. Song, and Z. Zeng, *J. Chem. Phys.* **135**, 044703 (2011).
- ⁵⁴ X. H. Zheng, X. L. Wang, Z. X. Dai, Z. Zeng, *J. Chem. Phys.* **134**, 044708 (2011).
- ⁵⁵ In Ref. 56, it has been shown how, in the case of transport through alkyl chains, the occupied levels shifts up in energy as the transverse supercell size is increased. Our model, based on cluster calculations, considers a completely isolated molecule on a gold electrode, which would be best compared with a larger supercell than the one used in Ref. 52.
- ⁵⁶ M. Strange and K. S. Thygesen, *Beilstein J. Nanotechnol.* **2**, 746 (2011).